Research Square

Preprints are preliminary reports that have not undergone peer review.
They should not be considered conclusive, used to inform clinical practice,
or referenced by the media as validated information.

Establishment and parameter calibration of double-layer bonded discrete element model for alfalfa stems at optimal harvest stage

Wei Zhang
Inner Mongolia University of Technology
Haitang Cen
haitang_cen@sina.com
Inner Mongolia University of Technology
Wang Guo
Inner Mongolia Academy of Science and Technology
Penghui She
Inner Mongolia University of Technology

Article

Keywords: Alfalfa stem, Optimal harvest stage, DEM, Double-layer bonded model, Parameter calibration

Posted Date: July 9th, 2026

DOI: https://doi.org/10.21203/rs.3.rs-10153236/v1

License: This work is licensed under a Creative Commons Attribution 4.0 International License.
Read Full License

Additional Declarations: No competing interests reported.

Establishment and parameter calibration of double-layer bonded discrete element model for alfalfa stems at optimal harvest stage

Wei Zhang[1], Haitang Cen[2*], Wang Guo[3], and Penghui She[2]

[1] School of Mechanics and Aeronautics, Inner Mongolia University of Technology, Hohhot 010051, China, zw24@imau.edu.cn

[2] School of Mechanical Engineering, Inner Mongolia University of Technology, Hohhot 010051, China

[3] Inner Mongolia Academy of Science and Technology, Hohhot 010000, China

[*] Correspondence: haitang_cen@sina.com; Tel.:+86-13514712360

Accurate discrete element method (DEM) modelling of alfalfa stems is essential for simulating cutting, conveying, stacking, and drying pre-treatment operations. However, conventional DEM models generally treat crop stems as homogeneous materials, thereby neglecting the structural heterogeneity between the epidermis and inner core. This study aimed to establish and calibrate a double-layer bonded DEM model for alfalfa stems at the optimal harvest stage. The physical, mechanical, and contact parameters of alfalfa stems were experimentally measured. A double-layer model comprising epidermis and inner-core regions was developed using the Hertz–Mindlin with Bonding (HMB) contact model. The key bonding and contact parameters were calibrated through Plackett–Burman screening, steepest ascent tests, and Box–Behnken response surface methodology. In addition, a feedforward neural network (FNN) was employed to predict the simulated shear force. The measured average moisture content, shear force, and repose angle were 0.723 ± 0.044 kg/kg, 56.36 N, and 31.62°, respectively. The shear-force response surface model achieved an R^2 of 0.9036, while the FNN model yielded an R^2 of 0.9077 and an RMSE of 0.9407. The results from the shear force response surface model and the FNN model are similar. The calibrated DEM model produced a simulated repose angle of 31.46°, corresponding to a relative error of only 0.51%. These results indicate that the proposed double-layer bonded DEM model can accurately represent the anisotropic mechanical behavior of alfalfa stems and provide a reliable simulation basis for optimizing alfalfa harvesting and drying pre-treatment equipment.

Keywords Alfalfa stem, Optimal harvest stage, DEM, Double-layer bonded model, Parameter calibration

Medicago sativa L. (alfalfa), a perennial herbaceous plant of the Leguminosae family, is hailed as the "King of Forages"due to its high stem and leaf nutritional density, excellent palatability, and strong environmental adaptability[1,2]. Its unique agronomic traits, superior nutritional value, and remarkable adaptability have been widely recognized globally[3], and it is currently extensively cultivated in Northeast, North, and Northwest China. With the continuous expansion of alfalfa planting areas, there is an urgent demand for efficient, low-loss technologies in key processes such as mechanized harvesting and crushing. However, the current alfalfa harvesting process still faces technical bottlenecks, including rapid cutting tool passivation and unreasonable mechanical parameter regulation, which severely restrict improvements in harvesting efficiency and product quality. Cutting and

crushing devices are core components for full-process alfalfa mechanization, and shearing is an indispensable key procedure. Establishing a high-fidelity DEM of alfalfa straw and simulating its shearing process can provide important theoretical support and technical reference for optimizing key components of alfalfa harvesting equipment, and is vital for advancing mechanized alfalfa processing technology.

With the rapid development and wide application of computer numerical simulation technology, DEM has become an essential approach to analyze the mechanical properties of crops and reveal their intrinsic dynamic laws[4,5]. This method can effectively characterize the contact behaviors between crops and mechanical components, including force, displacement, velocity and other physical parameters, and clarify the particle motion mechanism, thereby providing a solid theoretical basis for structural design and parameter optimization of agricultural machinery[6-8]. At present, the HMB contact model has been widely adopted by scholars to establish discrete element models for various crops, such as corn straw[9,10], pepper stems[11], rapeseed stalks[12,13], flax stems[14] and various crop seeds[15-18]. In terms of verification on crop mechanical characteristics, Zhao et al. established a discrete element model of cotton stalks using the HMB model, whose results verified the applicability of this model in analyzing particle wear characteristics and confirmed that it can accurately reproduce the mechanical response of cotton stalks during agricultural machinery operations[19]. Given that traditional linear elastic models and classic Hertz contact models are only suitable for simulating small deformation of crop stalks, Leblicq et al. constructed an improved DEM contact model based on experimental measured data, which incorporated plastic deformation and damage evolution effects; the validity of the proposed model was verified at both single-stalk and group levels, greatly improving the simulation accuracy of agricultural machinery operation processes[20]. Sun proposed a universal DEM modeling method for mature wheat plants and established flexible and breakable wheat plant models, which provides effective technical support for simulation analysis of wheat harvesting operations[21]. Li established a breakable corn ear model with the HMB contact model and accurately simulated the fragmentation law of corn ears in threshing components, further proving the great application potential of such bonding models in the numerical simulation of crop processing processes[22]. With regard to parameter calibration and experimental validation, Adajar calibrated the shear characteristics of stalks from five typical crops including rapeseed, corn and wheat, and the relative error between simulated and measured values was less than 2%[23]; Schramm et al. calibrated the elastic modulus and Poisson's ratio of wheat straw via DEM simulation, and the relative error between simulation results and physical test data was only 3.11%, fully demonstrating the reliability of the DEM simulation method[24]. Chevanan et al. conducted chopping experiments and shear strength tests on corn straw using a universal testing machine equipped with direct shear units, and it was found that crushed corn straw materials possess peak angular friction characteristics without obvious yield strength[25].

In existing simulation studies on breakable models, crop materials are typically treated as isotropic bodies and simplified into a single organizational structure, followed by the construction of bonded homogeneous particle models[26]. However, research on calibrating straw mechanical properties using double-layer bonded models remains relatively scarce. Previous studies have established a discrete element model for alfalfa stems at the budding stage based on the Hertz-Mindlin (no slip) model and conducted associated experiments, approximating alfalfa stems as cylinders composed of a single material[27]. In reality, alfalfa stems comprise three distinct components: thick-walled mechanical tissue, parenchyma cell tissue, and reticular vascular tissue, with significant material anisotropic characteristics between the outer epidermis and inner core[28]. Utilizing

homogeneous particles for simulation introduces considerable errors, which in turn impairs the reliability of simulation results. Meanwhile, the Hertz-Mindlin (no slip) model is commonly regarded as an integral model in the discrete element simulation software (EDEM), enabling effective simulation analysis and optimal design of processes such as transportation, grading, and sowing. Thus, there is an urgent necessity to develop a discrete element model capable of characterizing the separation process between the outer epidermis and inner core of alfalfa stems, while being suitable for simulating shearing behaviors.

Focusing on alfalfa stems at the optimal harvest stage, this study adopts the HMB model to establish the discrete element model of alfalfa stems and calibrate the simulation parameters, based on the differences in mechanical properties between the outer epidermis and inner core. This model enables parallel bonding of adjacent particles at their contact points, which is employed to simulate the interaction forces between the outer epidermis and inner core of the stems, with the simulation bonding parameters further calibrated. The accuracy of the alfalfa stem model and the effectiveness of the calibrated parameters are validated through both mechanical tests and simulation experiments. The research findings are intended to provide a scientific basis for the design and improvement of high-efficiency, low-loss alfalfa harvesting equipment.

Materials and methods

Experimental materials

The alfalfa used in this experiment was collected from Hohhot, Inner Mongolia, China (40°08′N, 111°31′E, altitude: 1000–1100 m; solar irradiance: 258.8–260.9W/m²), as shown in Fi. 1. The collected alfalfa had no obvious mechanical damage or pests and diseases, and was mowed in the natural state at the optimal harvest stage with a stubble height of 5–8 cm, followed by the removal of branches and leaves. The determination of the initial moisture content of alfalfa stems is a key step in analyzing contact parameters and mechanical property parameters, which helps ensure the accuracy of the parameters. In accordance with the GB/T 6435-2014 standard, five alfalfa stem samples (50 g each) were taken and dried in an oven (Model: DHG-245A; Shanghai Yiheng Scientific Instruments Co., Ltd.) at 105℃±2℃ for 24 hours. To ensure the accuracy of the test results, all samples were weighed using a calibrated balance during collection and pretreatment, and fully mixed before drying. The calculation formula for the initial moisture content of alfalfa stems is as follows:

$$M_0 = \frac{G_1 - G_0}{G_1} \quad (1)$$

Where M_0 is the initial moisture content of fresh alfalfa (kg/kg), G_1 is the mass of fresh alfalfa before drying (kg), and G_0 is the mass of alfalfa after drying (kg).



Fig. 1. Alfalfa plant

Measurement of physical properties of alfalfa stems at harvest stage

Geometric dimension measurement

Fifty alfalfa stems were randomly selected. Their diameter and length were measured using a digital caliper with 0.01 mm precision (Model 034299; Yantai Lvyi Tools Co., Ltd., China).

Density measurement

The density of alfalfa stems was measured using an automatic true density analyzer (Model G-DenPyc-3900M; CIQTEK Co., Ltd., Hefei, China), as shown in Fig. 2. Five 2 g samples were prepared for density testing.

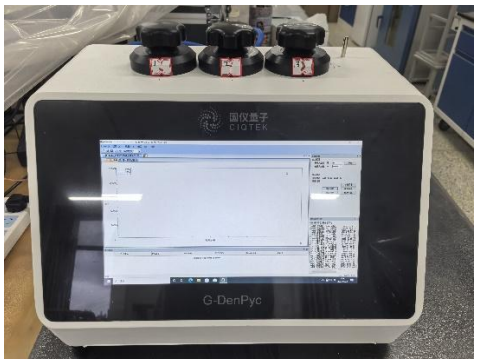


Fig. 2. Density measurement process of alfalfa stems

Poisson's ratio and shear modulus

Ten alfalfa stem samples were randomly selected and tested for mechanical properties using a TMS-Pro type material property analyzer (TMS-PRO; FTC). During the test, radial compressive load was applied to the stem samples until structural deformation became stable, with a constant loading speed of 30 mm/min. The radial deformation was recorded by the texture analyzer, while the axial deformation was measured using a digital vernier caliper (Model: 034299, Yantai Lvyi Tools Co., Ltd.). The calculation formula for Poisson's ratio of alfalfa stems is given as follows:

$$\varepsilon = \frac{|e\prime|}{|e|} = \frac{W_1 - W_0}{L_1 - L_0} \quad (2)$$

where ε denotes the Poisson's ratio of alfalfa stem, e' is the longitudinal deformation (mm), and e represents the transverse deformation (mm). W_1 and W_0 are the longitudinal lengths before and after loading (mm), while L_1 and L_0 are the transverse lengths before and after loading (mm).

Shear modulus is defined as the ratio of shear stress to shear strain under shear loading, which reflects the capability of materials to resist shear deformation. The corresponding calculation formula is presented as follows:

$$G = \frac{E}{2(1+\varepsilon)} \quad (3)$$

where G is the shear modulus of alfalfa stems, E is the elastic modulus of alfalfa stems, and ε is the Poisson's ratio of alfalfa stems. A TMS-Pro texture analyzer (TMS-PRO; FTC) was used to perform multiple tensile tests on alfalfa stem samples, and the average shear modulus of alfalfa stems was calculated using the above formula.

Measurement of contact parameters of alfalfa stems at optimal harvest stage

The measured contact parameters in this study consist of static friction coefficient and coefficient of restitution between alfalfa stem and steel plate, as well as between adjacent alfalfa stems.

Static friction coefficient

A CNY-1 inclined plane tester (Alpha Electronic Equipment Co., Ltd.) and a digital inclinometer with an accuracy of ±0.2° were adopted for the measurement. Auxiliary experimental facilities included a steel plate with dimensions of 250 mm × 100 mm × 2 mm and a self-made alfalfa stem plate, as illustrated in Fig. 3.

For the static friction test between alfalfa stems and steel plate, the steel plate was fixed on the inclined platform, and alfalfa stems were placed on the steel surface with their axial direction parallel to the platform length. The platform was kept horizontal initially and then tilted slowly. Once the stems tended to slide down, the inclination angle was recorded immediately. When measuring the static friction coefficient between alfalfa stems, the steel plate was replaced with the prepared alfalfa stem plate, and all other experimental procedures remained unchanged. The calculation formula of static friction coefficient is shown below.

$$\mu = tan\theta \quad (4)$$

Where μ represents the static friction coefficient, and θ is the critical sliding angle (°). Each test was repeated five times to obtain the static friction coefficients between alfalfa stems and steel plates, as well as between alfalfa stems.



Fig. 3. Measurement process of static friction coefficient

Coefficient of restitution

The coefficient of restitution between alfalfa stems and steel plate, as well as between adjacent alfalfa stems, was measured by the free-fall test method. During the test, alfalfa stems were freely released from an initial height of H_1 to perform free-fall motion, and rebounded after colliding with the steel plate placed below. A POC.dimax S high-speed camera was used to capture the rebound height H_0 of alfalfa stems, which was then analyzed and processed using TEMA 3.4-500 software. The coefficient of restitution was calculated based on the initial falling height H_1 and the measured rebound height H_0 of alfalfa stems, as shown in Fig. 4. For the measurement of the coefficient of restitution between alfalfa stems, the steel plate was only replaced with a self-made alfalfa stem plate, and all other experimental procedures were consistent with those for measuring the coefficient of restitution between alfalfa stems and steel plate. The calculation formula of the coefficient of restitution is as follows:

$$e = \sqrt{\frac{H_0}{H_1}} \quad (5)$$

where e denotes the restitution coefficient, H_1 is the initial free-fall height of alfalfa stems, and H_0 refers to the rebound height after collision. Each group of tests was repeated five times to acquire the restitution coefficients between alfalfa stems and steel plates as well as among alfalfa stems.

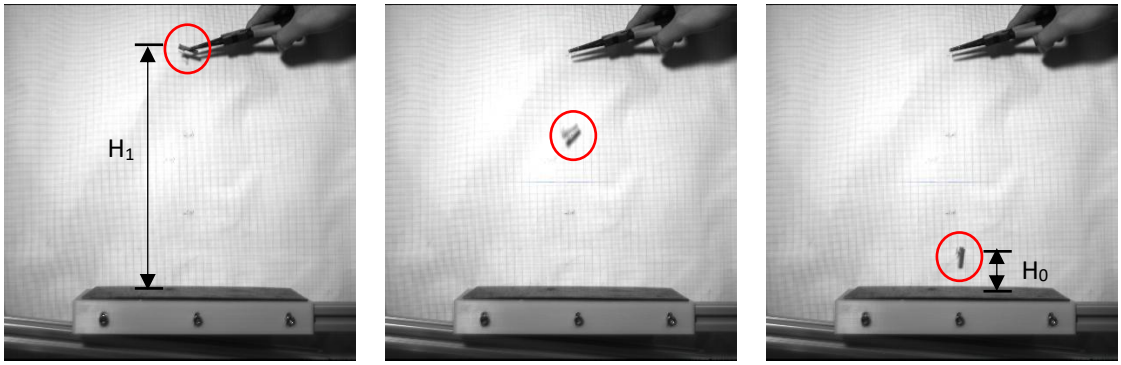


Fig. 4. Test procedure for restitution coefficient measurement

Angle of repose

The angle of repose is a crucial parameter that reflects the flowability and frictional properties of materials, and also serves as a key indicator for calibrating the contact characteristics of materials, which is conducive to obtaining more accurate simulation results. In this study, an FT-104B angle of repose tester was employed to determine the angle of repose of alfalfa stems. Fifty grams of alfalfa stem samples with a length of 60 mm were placed into the funnel of the tester, uniformly stirred, and then allowed to fall freely into the tray below. This operation was repeated 5 times. Each time, photos of the angle of repose were taken from the same position. MATLAB software was utilized to perform grayscale and binarization processing on the captured images, followed by contour extraction of the angle of repose. Finally, the angle of repose was measured using the software, as illustrated in Fig. 5.



Fig. 5. Measurement of angle of repose

Shear mechanical physical test

Shear tests on alfalfa stems were carried out using a TMS-PRO texture analyzer (FTC) to acquire experimental reference values for bonding parameter calibration, as shown in Fig. 6. Alfalfa stem specimens with a length of 60 mm and an average diameter of 3.4 mm were placed on a stationary support platform. The shear cutter moved downward at 20 mm/min with a compression ratio of 60%. Data acquisition was triggered once the cutter contacted the stem, and data were recorded every 0.1 s. All tests were repeated ten times.

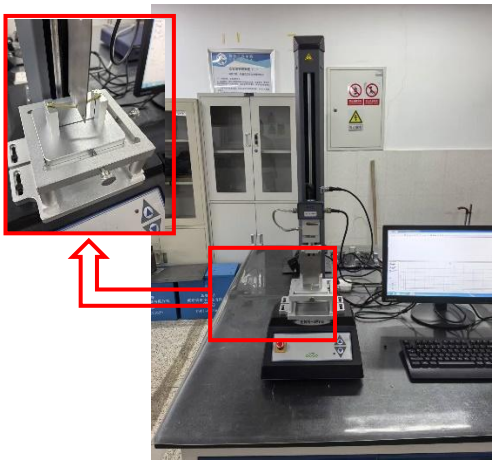


Fig. 6. Shear mechanical physical test

Alfalfa stem model construction

Bonding model destruction criteria

The HMB contact model was proposed by POTYONDY et al.[29], initially developed for simulating rock fragmentation, and later further improved and refined by many scholars to be applicable to the simulation of fragmentation and fracture behaviors of various materials. This model consists of multiple mutually bonded particles, which can form a bonded particle system with certain mechanical strength. The core principle is as follows: when the distance between the centers of two particles is less than the sum of their contact radii, the Bonding generation mechanism is automatically triggered, as shown in Fig. 7, thereby forming a bonded particle system with stable mechanical properties.

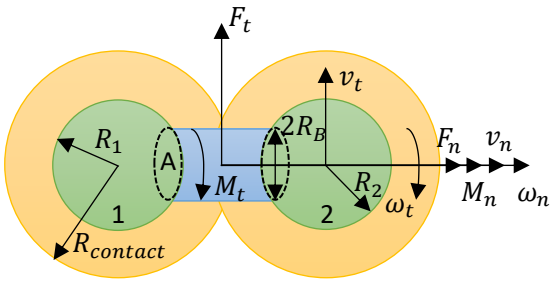


Fig. 7. Formation mechanism of internal bond bonds

Within each computational time step, the bond is subjected to both force and moment. The effect of this action accumulates with the increase of time steps, enabling the bond to resist external forces and generate deformation. The bond will fracture when the applied stress exceeds the critical stress, after which no bonding effect exists between particles. The relevant calculations are shown in Equations (6) to (9).

$$\begin{cases} \delta F_n = -v_n S_n A \delta t \\ \delta F_t = -v_t S_t A \delta t \\ \delta M_n = -\omega_n S_t J \delta t \\ \delta M_t = -\omega_t S_n \frac{J}{2} \delta t \end{cases} \tag{6}$$

$$\begin{cases} \sigma_{max} = \frac{-F_n}{A} + \frac{2M_t}{J} R_B \\ \tau_{max} = \frac{-F_t}{A} + \frac{2M_n}{J} R_B \end{cases} \tag{7}$$

$$\begin{cases} A = \pi R_B^2 \\ J = \frac{1}{2}\pi R_B^4 \end{cases} \quad (8)$$

$$R_B = \lambda \cdot \min(R_1, R_2) \quad (9)$$

Where δF_n and δF_t are the normal force and tangential force in a single time step (N), respectively; δM_n and δM_t are the normal moment and tangential moment in a single time step (N·m), respectively; v_n and v_t are the normal velocity and tangential velocity (m/s), respectively; ω_n and ω_t are the normal angular velocity and tangential angular velocity (rad/s), respectively; S_n and S_t are the normal stiffness per unit area and tangential stiffness per unit area (N/m^3), respectively; δt is the time step; J is the moment of inertia (m^4); σ_{max} and τ_{max} are the critical normal stress and critical tangential stress (Pa), respectively; A is the cross-sectional area of the Bond; λ is the bond radius coefficient; R_B is the bond radius (mm); R_1 is the physical radius of particle 1 (mm); and R_2 is the physical radius of particle 2 (mm).

Construction of discrete element model of alfalfa stems

The bonding model requires no overlap between adjacent particles, so the conventional automatic filling method based on particle templates is inapplicable. Regular and ordered particle arrangement is similar to crystal structure, which exhibits obvious anisotropic mechanical properties in all directions. For convenient modeling, the alfalfa stem was approximated as a cylindrical structure in this study. To balance computational complexity and model representativeness and accurately reflect the mechanical behavior of alfalfa stems, the stem was simplified into two composite structural layers, namely outer cortex and inner core. Previous studies have established multi-layer particle bonding models according to the mechanical property differences between outer layer and inner core of agricultural products, including corn straw[10], ramie stalk[30], pepper stem[11], Chinese cabbage root[31] and yam[8]. These existing studies provide effective references for establishing the discrete element model of alfalfa stems.

Considering the obvious differences in morphology and structure between the outer cortex and inner core of alfalfa stems, the stem specimens with a diameter of 3 mm and a length of 60 mm were adopted for shear tests. In this study, the three-dimensional coordinate method was applied to accurately establish the physical structure with a limited number of particles. A rectangular coordinate system OXYZ was established via SolidWorks software, in which the XOY plane was defined as the cross-section of the alfalfa stem, the Z-axis was aligned with the stem axial direction, and the origin O(0,0,0) was set as the geometric center of the cross-section. The centroid coordinates of particles in the first layer were determined, and particles of subsequent layers were arranged at an interval of 0.4 mm along the Z-axis. Then all coordinate data were imported into EDEM software. In the established model, each layer was arranged with 56 particles, and the particle number gradually decreased from the outer layer to the inner layer to ensure no overlap among particles. To form stable bonding contacts between outer cortex and inner core particles, spherical particles with a diameter of 0.4 mm were used to construct the outer cortex, while particles ranging from 0.3 mm to 0.35 mm were employed to fill the inner core region. Ultimately, the established discrete element model of alfalfa stem consisted of 7946 particles in total.

Shear mechanics simulation test

The models of shear cutter and test bench were established by using SolidWorks and exported into STL files. The alfalfa stem model was generated in EDEM, and the file of New Simulation Deck was exported in post-processing module with the initial simulation time set as 0.01 s. Subsequently, the STL files of cutter and bench were imported into the New Simulation Deck and arranged at reasonable positions, and then loading was applied to the alfalfa stem model.

The shear simulation test was terminated once the alfalfa stem fractured, as shown in Figure 8. Previous studies have proven that loading rate exerts negligible influence on simulation results [32], so the fixture loading rate was set to 1 mm/s in this shear simulation. To guarantee simulation accuracy, the fixed time step was defined as 1×10^{-6} s, accounting for 15.32% of the Rayleigh time step, and the data recording interval was set to 0.001 s. The whole process of the established shear simulation test for alfalfa stems is presented in Fig. 8.

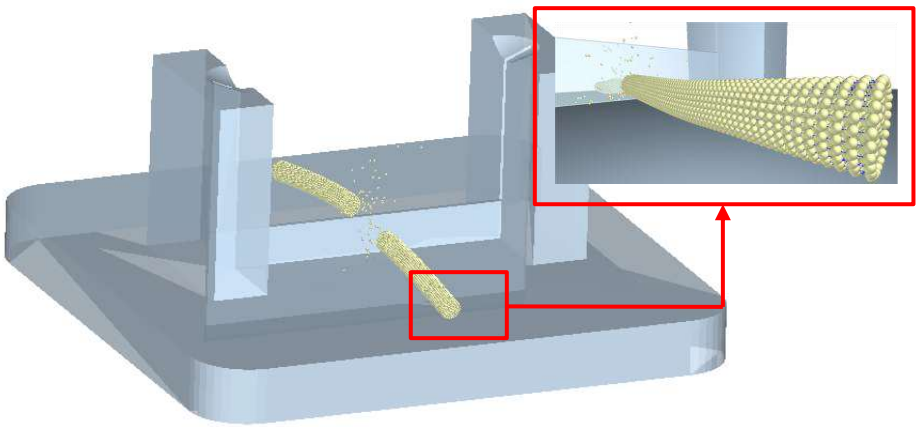


Fig. 8. Simulation shear mechanical test of alfalfa stems

Angle of repose simulation test

A three-dimensional model of the angle of repose measuring device was established using SolidWorks software. After structural simplification, the model was imported into the EDEM platform for simulation calibration. The Edinburgh Elasto-Plastic Adhesion (EEPA) contact model was selected in the calibration process, and alfalfa stem particles were dynamically generated through the particle factory. The particle factory was configured to produce particles uniformly in time and space to ensure the homogeneous distribution of alfalfa stems. A total of 300 alfalfa stem models with a diameter of 3 mm and a length of 60 mm were introduced into the simulation domain within 3 seconds. The simulation was terminated when the stems settled completely and formed a stable accumulation at the bottom of the hopper. The stacking morphology images were captured and processed in MATLAB to extract and fit the contour curves, based on which the simulated angle of repose was calculated. The simulation device and numerical model for the angle of repose test are shown in Fig. 9.

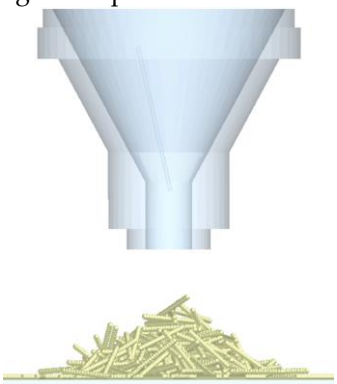


Fig. 9. Simulation test of repose angle for alfalfa stems

Regression prediction of Shear Force based on FNN

Based on the significant factors affecting shear force identified through response surface methodology (RSM), a fully connected FNN was developed in MATLAB to predict the shear

force of alfalfa stems. The network was trained using the Levenberg–Marquardt optimization algorithm, which enables rapid iterative updating of weights and biases. The hyperbolic tangent sigmoid function (Tansig) was employed as the hidden-layer transfer function to enhance the capability of the model to capture nonlinear mapping relationships. The constructed FNN consisted of two hidden layers, with 20 and 10 neurons in the first and second hidden layers, respectively. After model training, the network outputs were inverse-normalized to obtain the predicted shear force of alfalfa stems.

A total of 30 experimental samples were obtained from the experiments and randomly divided into training, validation, and testing subsets at a ratio of 8:1:1. The predictive performance of the FNN model was quantitatively evaluated using the root mean square error (RMSE) and the coefficient of determination (R^2). RMSE was used to characterize the average deviation between the predicted and experimental values, with smaller values indicating lower prediction errors. R^2 was used to quantify the extent to which the model explained the variation in the experimental response, values closer to 1 indicate higher fitting accuracy and greater predictive reliability.

Results

Physical parameters of alfalfa stems

The basic physical and contact mechanical parameters of alfalfa stems were obtained through a series of physical measurement experiments. The measured results show that the average initial moisture content of alfalfa stems was 0.723±0.044 kg/kg, the average diameter was 3.41 mm, the average stem length was 529.35 mm, the average density was 994.46 kg/m^3, the average Poisson's ratio was 0.4, and the average shear modulus was 18.26 MPa. The collision restitution coefficients of alfalfa stem–steel plate and alfalfa stem–alfalfa stem were 0.32–0.64 and 0.25–0.5, respectively. The static friction coefficients for alfalfa stem–steel plate and alfalfa stem–alfalfa stem contact were 0.2–0.5 and 0.2–0.6, respectively. The average shear force of alfalfa stems was determined to be 56.36 N. The average repose angle of alfalfa stems was measured to be 31.62°. All the above measured parameters can provide reliable basic data for parameter calibration and numerical simulation of the discrete element model of alfalfa stems.

Calibration of shear force parameters

Screening of influencing factors for bonding parameters

The HMB model was adopted to describe the internal mechanical behavior of the alfalfa stem discrete element model. Its shear fracture characteristics are jointly governed by a series of bonding parameters. Conducting combinatorial optimization tests for all parameters would lead to a large number of experimental runs and severe parameter coupling effects, which greatly compromise the calibration efficiency. Accordingly, key parameters including bonding normal stiffness, tangential stiffness, critical normal stress and critical tangential stress were selected for screening based on the theoretical principle of the HMB model. Given the large number of bonding parameters to be calibrated, the epidermis and pith of alfalfa stems were simplified as isotropic materials according to a previous study[33]. In this case, the normal and tangential contact stiffness, as well as the critical normal and tangential stress, were assigned identical values for pith-pith and epidermis-epidermis contacts, respectively.

Following the above simplification, a total of eight parameters were determined as screening factors, namely the contact stiffness and critical stress of pith-pith, epidermis-epidermis and epidermis-pith interfaces. The Plackett-Burman screening test was performed using the deviation between simulated and measured shear failure forces as the evaluation index. The value ranges of all factors were referenced from published studies on typical stalk crops such as corn and rapeseed stalks[9,13]. The factor level settings, experimental schemes and results, as well as variance analysis results are presented in Table 1, Table 2 and Table 3, respectively.

Code	Simulation parameters	Low level -1	High level 1
x1	Epidermis–epidermis normal/tangential contact stiffness($N \cdot m^{-1}$)	1.2×10^{9}	5.8×10^{9}
x2	Epidermis–epidermis critical normal/tangential stress(Pa)	1.4×10^{8}	6.6×10^{8}
x3	Pith–pith normal/tangential contact stiffness($N \cdot m^{-1}$)	4.0×10^{6}	4.0×10^{7}
x4	Pith–pith critical normal/tangential stress(Pa)	1.0×10^{8}	1.0×10^{9}
x5	Epidermis–pith normal contact stiffness($N \cdot m^{-1}$)	2.0×10^{8}	2.0×10^{9}
x6	Epidermis–pith tangential contact stiffness($N \cdot m^{-1}$)	1.0×10^{8}	1.0×10^{9}
x7	Epidermis–pith critical normal stress(Pa)	1.0×10^{6}	6.0×10^{6}
x8	Epidermis–pith critical tangential stress(Pa)	8.0×10^{5}	1.0×10^{6}

Table 1. Coding of factors for Plackett-Burman test of bonding parameters

NO.	x1	x2	x3	x4	x5	x6	x7	x8	F（N）
1	-1	1	1	1	-1	-1	-1	1	71.68
2	1	1	-1	1	1	1	-1	-1	38.26
3	-1	1	-1	1	1	-1	1	1	67.81
4	-1	-1	1	-1	1	1	-1	1	39.54
5	1	1	1	-1	-1	-1	1	-1	66.34
6	1	-1	1	1	1	-1	-1	-1	39.61
7	-1	-1	-1	1	-1	1	1	-1	59.62
8	1	-1	-1	-1	1	-1	1	1	52.73
9	-1	-1	-1	-1	-1	-1	-1	-1	68.46
10	-1	1	1	-1	1	1	1	-1	36.51
11	1	1	-1	-1	-1	1	-1	1	71.35
12	1	-1	1	1	-1	1	1	1	56.18

Table 2. Scheme and results of Plackett–Burman test for bonding parameters

Parameters	Sum of squares	Degree of freedom	Mean square	F-value	P-value
Model	2091.30	8	261.41	16.17	0.0215*
x1	30.56	1	30.56	1.89	0.2629
x2	106.86	1	106.86	6.61	0.0824
x3	194.97	1	194.97	12.06	0.0403*
x4	0.26	1	0.26	0.0161	0.9069
x5	1183.46	1	1183.46	73.18	0.0034**
x6	353.93	1	353.93	21.89	0.0185*
x7	8.82	1	8.82	0.55	0.5136
x8	212.44	1	212.44	13.14	0.0361*
Residual	48.51	3	16.171475		
Cor Total	2139.82	11			

Table 3. Analysis of variance (ANOVA) of Plackett-Burman test for bonding parameters. ** indicates extremely significant difference ($p \leq 0.01$); * indicates significant difference ($0.01 < p < 0.05$). The same applies hereinafter.

Steepest ascent experimental design for bonding parameters

Following the Plackett-Burman screening of significant bonding parameters, the steepest ascent design was employed to rapidly approach the optimal value ranges of key parameters.

The experimental scheme and corresponding results are presented in Table 6. As the values of each significant parameter increased gradually, the simulated shear force acting on alfalfa stems by the cutting tool also increased accordingly. Meanwhile, the relative error between the simulated and measured shear failure forces first decreased and then increased. The parameter combination in NO. 4 yielded the minimum relative error, indicating that the optimal range was close to the conditions of NO. 4. Therefore, NO. 3 and 5 were selected as the low and high levels, respectively, and NO. 4 was chosen as the center point for the subsequent Box-Behnken response surface methodology.

NO.	x3	x5	x6	x8	Simulated shear force (N)	Relative error (%)
1	4.0×10^{6}	2.00×10^{8}	1.00×10^{8}	8.0×10^{5}	49.36	14.18
2	1.3×10^{7}	6.50×10^{8}	3.25×10^{8}	8.5×10^{5}	52.76	6.82
3	2.2×10^{7}	1.10×10^{9}	5.50×10^{8}	9.0×10^{5}	55.06	2.36
4	3.1×10^{7}	1.55×10^{9}	7.75×10^{8}	9.5×10^{5}	56.88	0.91
5	4.0×10^{7}	2.00×10^{9}	1.00×10^{9}	1.0×10^{6}	58.94	4.38

Table 4. Schemes and results of steepest ascent test for bonding parameters

Box–Behnken test results and analysis for bonding parameters

To further investigate the relationship between the shear force of alfalfa stems and the significant parameters x3, x5, x6, and x8, and to determine the optimal parameter combination, a Box-Behnken response surface methodology was designed based on the results of the steepest ascent test. The coded levels of each simulation parameter are presented in Table 5, and a total of 27 simulation runs were performed. The experimental design matrix and corresponding results are shown in Table 6.

Level	x3	x5	x6	x8
-1	2.2×10^{7}	1.10×10^{9}	5.50×10^{8}	9.0×10^{5}
0	3.1×10^{7}	1.55×10^{9}	7.75×10^{8}	9.5×10^{5}
1	4.0×10^{7}	2.00×10^{9}	1.00×10^{9}	1.0×10^{6}

Table 5. Coding of factors of response surface test for bonding parameters

NO.	x3	x5	x6	x8	Simulated shear force (N)
1	1	1	0	0	56.13
2	0	0	0	0	56.12
3	0	-1	0	-1	52.11
4	1	0	0	1	57.96
5	-1	1	0	0	55.79
6	0	-1	-1	0	54.12
7	0	1	1	0	57.27
8	0	0	0	0	56.25
9	-1	0	0	1	55.93
10	0	0	-1	-1	54.22
11	-1	-1	0	0	53.15
12	0	-1	0	1	57.77
13	-1	0	1	0	56.98
14	-1	0	-1	0	55.29
15	-1	0	0	-1	54.38
16	1	-1	0	0	55.39
17	0	1	-1	0	58.51

18	1	0	0	-1	52.19
19	0	0	1	1	59.52
20	0	0	-1	1	56.48
21	0	1	0	-1	55.34
22	0	1	0	1	57.53
23	0	0	1	-1	56.28
24	1	0	1	0	57.78
25	0	0	0	0	56.51
26	1	0	-1	0	56.62
27	0	-1	1	0	55.47
28	0	-1	0	1	56.82
29	-1	0	0	0	58.19

Table 6. Design and results of Box–Behnken experiment for bonding parameters

Box–Behnken test results and analysis for bonding parameters

The results of variance analysis for the Box-Behnken design are presented in Table 7. The F-value of the quadratic regression model is 9.38, and the model is highly significant ($p<0.0001$), indicating that it can effectively describe the relationship between parameters and shear force. Variables x5, x6 and x8 exerted an extremely significant effect on shear force ($p<0.01$), while quadratic term x3x8, x5x8 and $x6^2$ exhibited a significant influence ($p<0.05$). The remaining terms were statistically non-significant. The lack-of-fit test was non-significant ($p=0.2175$). The coefficient of determination R^2 is 0.9036 and the adjusted coefficient of determination $Radj^2$ is 0.8073, demonstrating that the model possesses strong explanatory power. The second-order regression equation for the shear force of alfalfa stems against various factors is established and expressed as Equation (10). The fitted equation after removing non-significant terms is presented in Eq. (11).

Source	Sum of Squares	Degree of freedom	Mean Square	F-value	P-value
Model	80.29	14	5.73	9.38	< 0.0001**
x3	1.20	1	1.20	1.97	0.1822
x5	14.00	1	14.00	22.89	0.0003**
x6	6.98	1	6.98	11.42	0.0045**
x8	37.39	1	37.39	61.13	< 0.0001**
x3 x5	0.9025	1	0.9025	1.48	0.2445
x3 x6	0.5652	1	0.5652	0.9242	0.3527
x3 x8	4.45	1	4.45	7.28	0.0173*
x5 x6	1.68	1	1.68	2.74	0.1200
x5 x8	3.46	1	3.46	5.66	0.0321*
x6 x8	0.2401	1	0.2401	0.3926	0.5410
$x3^2$	1.66	1	1.66	2.72	0.1216
$x5^2$	1.60	1	1.60	2.61	0.1283
$x6^2$	3.68	1	3.68	6.01	0.0279*
$x8^2$	0.8708	1	0.8708	1.42	0.2526
Residual	8.56	14	0.6116		
Lack of Fit	7.30	10	0.7300	2.31	0.2175
Pure Error	1.26	4	0.3155		
Cor Total	88.85	28			

Table 7. Design and results of Box–Behnken experiment for bonding parameters

$$Y1=-118.81-1.46*x3+5.52*x5-2.72*x6+0.0003*x8-1.17x3x5-1.7x3x6+2.34x3x8-6.4x5x6-3.79x5x8+2.18*x6x8-6.79x3^2-2.66x5^2+1.62*x6^2-1.59x8^2 \quad (10)$$

$$Y2=-118.81+5.52*x5-2.72*x6+0.0003*x8+2.34x3x8-3.79x5x8+1.62*x6^2 \quad (11)$$

Simulated shear force regression prediction based on FNN

After model training, the network outputs were inverse-normalized to obtain the predicted shear failure force of alfalfa stems. A scatter plot was then generated using the simulated shear force as the abscissa and the FNN-predicted shear force as the ordinate. Linear regression analysis was performed on the prediction results, with the ideal relationship line (y = x) introduced as a reference to evaluate the agreement between the model predictions and the simulated values, as shown in Fig. 10. The fitting results yielded a linear regression equation of y = 0.9526x + 2.6381, with R^2 = 0.9077 and RMSE = 0.9407. These results indicate that the developed FNN model achieved satisfactory prediction accuracy and fitting performance for the shear failure force of alfalfa stems.

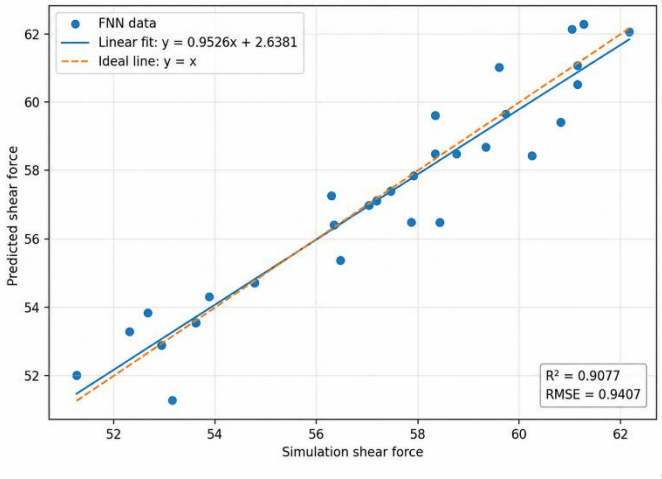


Fig. 10. Simulated shear force regression prediction based on FNN

Calibration of repose angle parameters

Screening of influencing factors for repose angle

To efficiently screen the physical parameters that significantly affect the repose angle of alfalfa stems, the Plackett-Burman test was conducted. Based on published literature[22,27] and preliminary physical experiments, nine factors were selected, including Poisson's ratio of alfalfa stems (X1), epidermis density (X2), epidermis shear modulus (X3), epidermis–epidermis restitution coefficient (X4), epidermis–steel plate restitution coefficient (X5), epidermis–epidermis static friction coefficient (X6), epidermis–steel plate static friction coefficient (X7), epidermis–epidermis rolling friction coefficient (X8) and epidermis–steel plate rolling friction coefficient (X9). The simulated repose angle was taken as the evaluation index. The factor levels, experimental design and results, as well as analysis of variance are presented in Table 8, Table 9 and Table 10, respectively.

Code	Simulation parameters	Low level -1	High level 1
X1	Poisson's ratio	0.26	0.5
X2	epidermis density (kg·m^{-3})	960	990
X3	epidermis shear modulus (MPa)	7	30
X4	epidermis–epidermis restitution coefficient	0.25	0.5
X5	epidermis–steel plate restitution coefficient	0.32	0.64
X6	epidermis–epidermis static friction coefficient	0.2	0.6
X7	epidermis–steel plate static friction coefficient	0.2	0.5

X8	epidermis–epidermis rolling friction coefficient	0.1	0.3
X9	epidermis–steel plate rolling friction coefficient	0.05	0.25

Table 8. Coding of factors for Plackett-Burman test of repose angle

NO.	X1	X2	X3	X4	X5	X6	X7	X8	X9	repose angle(°)
1	0.5	990	7	0.5	0.64	0.6	0.2	0.1	0.05	31.42
2	0.5	960	30	0.5	0.32	0.6	0.5	0.3	0.05	34.31
3	0.5	990	7	0.25	0.32	0.6	0.2	0.3	0.25	37.65
4	0.26	990	30	0.25	0.64	0.6	0.5	0.1	0.05	31.82
5	0.26	960	7	0.5	0.32	0.6	0.5	0.1	0.25	36.51
6	0.5	990	30	0.25	0.32	0.2	0.5	0.1	0.25	33.51
7	0.26	990	30	0.5	0.32	0.2	0.2	0.3	0.05	30.79
8	0.26	960	7	0.25	0.32	0.2	0.2	0.1	0.05	34.49
9	0.26	960	30	0.25	0.64	0.6	0.2	0.3	0.25	35.81
10	0.26	990	7	0.5	0.64	0.2	0.5	0.3	0.25	28.76
11	0.5	960	7	0.25	0.64	0.2	0.5	0.3	0.05	31.33
12	0.5	960	30	0.5	0.64	0.2	0.2	0.1	0.25	29.86

Table 9. Scheme and results of Plackett–Burman test for repose angle

Source	Sum of Squares	Degree of freedom	Mean Square	F-value	P-value
Model	84.92	9	9.45	36.13	0.0272
X1	0.0008	1	0.0008	0.0032	0.901
X2	5.82	1	5.82	22.31	0.0420*
X3	1.37	1	1.37	5.26	0.1488
X4	14.00	1	14.00	53.61	0.0181*
X5	27.79	1	27.79	106.42	0.0093**
X6	29.39	1	29.39	112.57	0.0088**
X7	1.19	1	1.19	4.56	0.1662
X8	0.0901	1	0.0901	0.3452	0.6163
X9	5.25	1	5.25	20.12	0.0463*
Residual	0.5222	2	0.2611		
Cor Total	85.43	11			

Table 10. Analysis of variance (ANOVA) of Plackett-Burman test for repose angle

Steepest ascent experimental design for repose angle

Based on the analysis of variance (ANOVA) results of the Plackett-Burman test for physical parameters of repose angle, epidermis density (X2), epidermis–epidermis restitution coefficient (X4), epidermis–steel plate restitution coefficient (X5), epidermis–epidermis static friction coefficient (X6) and epidermis–steel plate rolling friction coefficient (X9) had significant effects on the simulated repose angle ($p<0.05$), whereas the other parameters showed no significant differences ($p>0.05$). The three most influential factors X4, X5 and X6 were selected as experimental variables, and the remaining parameters were fixed at their intermediate levels. Taking the relative error between measured and simulated repose angles as the evaluation index, a steepest ascent test was conducted to quickly approach the optimal value ranges of the key parameters. The experimental design and results are shown in Table 11.

NO.	X4	X5	X6	Simulated repose	Relative error（%）

				angle(°)	
1	0.25	0.32	0.2	26.53	16.10
2	0.30	0.40	0.3	28.85	8.76
3	0.35	0.48	0.4	30.14	4.68
4	0.40	0.56	0.5	33.57	6.17
5	0.50	0.64	0.6	35.81	13.25

Table 11. Schemes and results of steepest ascent test for repose angle

Results and analysis of Box-Behnken test for repose angle

To further explore the relationships between the repose angle of alfalfa stems and the parameters X4, X5 and X6, and to determine their optimal combination, a Box-Behnken response surface experiment was designed based on the results of the steepest ascent test. The NO. 3 from the steepest ascent test was set as the central level, while NO. 2 and NO. 4 were defined as the low and high levels, respectively. A three-factor and three-level Box-Behnken design was adopted, with five replicated runs arranged at the central point, resulting in a total of 17 experimental runs. All other parameters remained consistent with those used in the steepest ascent test for repose angle-related physical parameters. The coded levels of the significant physical parameters are presented in Table 12, and the experimental design and corresponding results are listed in Table 13.

Level	X4	X5	X6
-1	0.30	0.40	0.3
0	0.35	0.48	0.4
1	0.40	0.56	0.5

Table 12. Coding of factors of response surface test for repose angle

NO.	X4	X5	X6	Repose angle(°)
1	0.4	0.4	0.4	31.21
2	0.35	0.48	0.4	34.14
3	0.35	0.48	0.4	32.92
4	0.35	0.56	0.5	34.87
5	0.35	0.48	0.4	33.05
6	0.3	0.56	0.4	30.24
7	0.3	0.48	0.3	28.11
8	0.35	0.4	0.3	30.08
9	0.35	0.4	0.5	33.79
10	0.3	0.4	0.4	30.26
11	0.35	0.48	0.4	33.11
12	0.35	0.56	0.3	30.32
13	0.4	0.56	0.4	32.84
14	0.4	0.48	0.5	34.01
15	0.35	0.48	0.4	33.02
16	0.3	0.48	0.5	31.98
17	0.4	0.48	0.3	30.59

Table 13. Design and results of Box–Behnken experiment for repose angle

The ANOVA results of the Box-Behnken test are presented in Table 14. The quadratic regression model yielded an F-value of 33.48, which was highly significant ($p<0.0001$),

indicating that the model could effectively describe the relationship between the parameters and the repose angle. X4, X6 and quadratic term $X4^2$ exerted an extremely significant effect on the angle of repose ($p<0.01$), while linear term X5 and quadratic term $X5^2$ exhibited a significant influence ($p<0.05$). The remaining terms were statistically non-significant.

The lack-of-fit test was non-significant ($p=0.8118$). The coefficient of determination ($R^2=0.9773$) indicated that the model could explain 97.73% of the variation in the repose angle. The adjusted coefficient of determination ($Radj^2=0.9481$) further confirmed the strong explanatory power of the model after accounting for the number of variables. A second-order regression equation relating the simulated repose angle of alfalfa stems to the tested factors was obtained, as shown in Eq. (12). The fitted equation after removing non-significant terms is presented in Eq. (13).

Source	Sum of Squares	Degree of freedom	Mean Square	F-value	P-value
Model	54.09	9	6.01	33.48	< 0.0001**
X4	8.12	1	8.12	45.23	0.0003**
X5	1.07	1	1.07	5.98	0.0444*
X6	30.23	1	30.23	168.35	< 0.0001**
X4 X5	0.6806	1	0.6806	3.79	0.0926
X4 X6	0.0506	1	0.0506	0.2820	0.6118
X5X6	0.1764	1	0.1764	0.9825	0.3546
$X4^2$	10.80	1	10.80	60.15	0.0001**
$X5^2$	1.09	1	1.09	6.08	0.0432*
$X6^2$	0.9460	1	0.9460	5.27	0.0554
Residual	1.26	7	0.1795		
Lack of Fit	0.2433	3	0.0811	0.3201	0.8118
Pure Error	1.01	4	0.2534		
Cor Total	55.35	16			

Table 14. Design and results of Box–Behnken experiment for repose angle

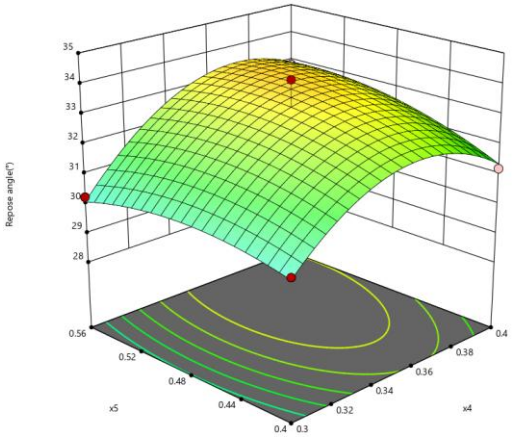
$$\theta1=-68.94+428.07*X4+34.33*X5+52.63*X6+103.13*X4X5-22.5*X4X6+26.25X5X6-640.6*X4^2-79.53*X5^2-47.4*X6^2 \quad (12)$$

$$\theta2=-68.94+428.07*X4+34.33*X5+52.63*X6-640.6*X4^2-79.53*X5^2 \quad (13)$$

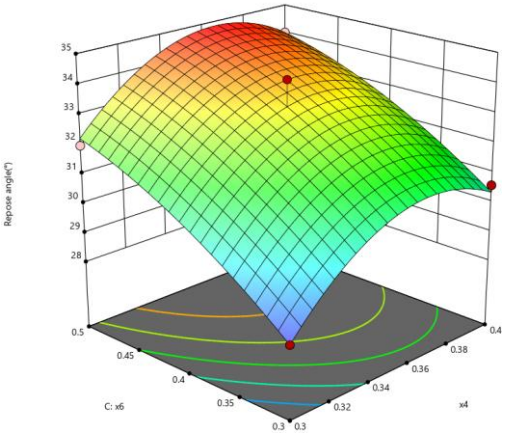
The response surfaces illustrating the interactive effects of various factors on the repose angle of alfalfa stems are presented in Fig. 11, which includes the response surface and contour plots for the three pairs of factors: X4-X5, X4-X6, and X5-X6. Overall, all three sets of response surfaces exhibit a distinct dome-shaped profile, indicating that within the investigated ranges of the factors, the repose angle shows a non-linear response that first increases and then decreases with the variation of any two factors.

As shown in Fig. 11(a), the repose angle reaches its peak near the combination of medium-to-high levels of both X4 and X5, and decreases as the levels of both factors deviate towards either end of their respective ranges. Fig. 11(b) reveals that the peak of the response surface is located in the region corresponding to a low level of X4 and a high level of X6, with a steeper gradient along the X6 direction, suggesting that X6 exerts a relatively greater influence on the repose angle. As shown in Fig. 11(c), the peak of the response surface is skewed towards the high levels of both X5 and X6, and the overall trend of the surface is the steepest, indicating that the interaction between these two factors has the most sensitive regulatory effect on the repose angle, with even small deviations in their levels leading to a noticeable reduction in the repose angle.

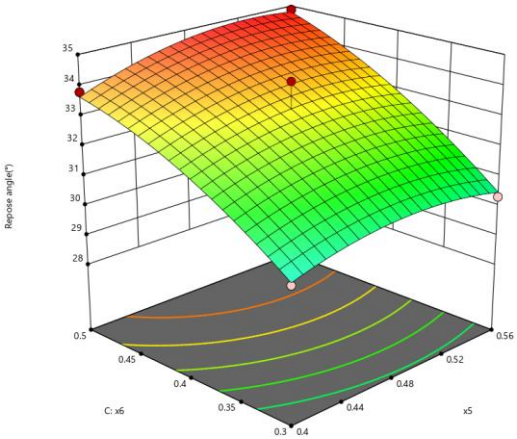
Collectively, the interactive effects of all three factor pairs are critical determinants of the repose angle of alfalfa stems, with distinct differences in their response patterns and sensitivity. Among these, the interaction between X5 and X6 exhibits the most significant regulatory effect on the repose angle.



(a)Y=f(X4, X5)



(b) Y=f(X4, X6)



(c) Y=f(X5, X6)

Fig. 11. Effects of two-factor interactions on the repose angle

Simulation test verification of repose angle

To verify the accuracy and feasibility of the calibrated physical parameters, the optimal combination was adopted for parameters that significantly affect the angle of repose, and the median values within the ranges measured by physical tests were used for non-significant parameters. A total of five repeated simulation tests on the angle of repose were conducted,

and the corresponding parameter values are listed in Table 15. The average simulated angle of repose was 31.46°, with a relative error of 0.51% compared with the average value from physical tests. The results show a good agreement between simulation and physical measurement, which demonstrates that the calibrated physical parameters for alfalfa stems are accurate and reliable.

Simulation parameters	Value
alfalfa stem Poisson's ratio	0.38
alfalfa stem density (kg·m^{-3})	975
alfalfa stem shear modulus (MPa)	18.5
steel Poisson's ratio	0.30
steel density (kg·m^{-3})	7850
steel shear modulus (MPa)	7.0×10^{10}
epidermis–epidermis restitution coefficient	0.38
epidermis–steel plate restitution coefficient	0.44
epidermis–epidermis static friction coefficient	0.32
epidermis–steel plate static friction coefficient	0.35
epidermis–epidermis rolling friction coefficient	0.2
epidermis–steel plate rolling friction coefficient	0.15

Table 15. Design and results of Box–Behnken experiment for repose angle

Discussion

Numerical simulation techniques have greatly facilitated the design and performance optimization of agricultural equipment. In simulation analyses, prediction accuracy and computational efficiency are always the primary concerns. Most existing DEM models for crop stems simplify plant tissues into homogeneous and isotropic cylindrical structures. Such models ignore the substantial differences in microstructure and mechanical properties between the outer epidermis and inner core, which inevitably leads to large deviations between simulated results and actual mechanical responses[34, 35].

Considering the material heterogeneity between the mechanical tissue of the epidermis and the parenchyma-vascular bundle tissue of the inner core of alfalfa stems at the harvest stage, a double-layer bonded DEM model consisting of an epidermis layer and an inner core layer was established in this study. Spherical particles with different sizes were used to fill the epidermis and inner core regions, and the HMB contact model was adopted to characterize the mechanical interactions within each layer and between the two layers. Compared with the conventional homogeneous modelling method, the proposed double-layer structure can faithfully reproduce the layered configuration of alfalfa stems. It effectively simulates the synergistic deformation, fracture and separation behaviours between the epidermis and inner core during shearing and stacking processes, and overcomes the limitation of homogeneous models in describing the anisotropic mechanical properties of stems. Following the layered modelling strategies reported for agricultural and forestry biomass materials such as corn stalks and rapeseed stems[10, 13], particles were regularly arranged via the spatial coordinate positioning method. This arrangement ensures no particle overlap while balancing computational efficiency and simulation accuracy. The presented modelling framework and structural division method can serve as a reference for constructing DEM models of stems of similar herbaceous crops.

DEM involves numerous parameters with strong coupling effects. Calibrating all parameters through full-factor combination tests is extremely labor-intensive and inefficient. In this work, a stepwise calibration strategy combining Plackett–Burman screening test, steepest ascent test and RSM was proposed. Firstly, key parameters that significantly affect the

Shear Force and angle of repose were screened out from 8 bonding parameters and 9 contact parameters. Secondly, the steepest ascent test was conducted to rapidly approach the optimal parameter range. Finally, a second-order regression model between parameters and response indicators was established using RSM, achieving efficient and accurate calibration of multiple parameters. The present findings are consistent with previous studies on the stacking characteristics of crop stalks and ranular materials[17, 36].

Several limitations of this study should be acknowledged. First, all experiments were performed using alfalfa stems at the harvest stage with a single moisture content and plant type. The mechanical and stacking characteristics of stems at different growth stages, varying moisture contents, lodged stems and stems with different diameters were not investigated. Second, the current simulations only focused on static shear tests and static angle of repose tests, and the model applicability under complex working conditions, including high-speed impact, dynamic conveying, cutting and crushing, remains unvalidated. Future work will conduct parameter calibration for alfalfa stems at different growth stages and moisture contents, and revise the model based on tests under diverse working conditions. Furthermore, intelligent algorithms such as neural networks will be adopted to improve the accuracy of parameter inversion. This study is expected to provide comprehensive simulation support for the optimal design of key components of alfalfa harvesting machinery.

Conclusions

1. The basic physical and contact parameters of alfalfa stems at the optimal harvest stage were systematically determined through laboratory experiments. The average moisture content, diameter, density, Poisson's ratio, and shear modulus were 0.723 kg/kg, 3.41 mm, 994.46 kg/m^3, 0.4, and 18.26 MPa, respectively. The coefficients of restitution for stem–steel plate and stem–stem contacts were 0.39–0.52 and 0.25–0.34, respectively, while the corresponding static friction coefficients were 0.36–0.54 and 0.32–0.64. The measured average angle of repose was 31.62°. These experimentally measured parameters provide reliable basic data for DEM model construction and parameter calibration of alfalfa stems at the optimal harvest stage.
2. A double-layer bonded DEM model consisting of an epidermis layer and an inner core was developed to represent the structural heterogeneity and anisotropic mechanical behavior of alfalfa stems. The model contained 7946 particles, with 0.4 mm particles used for the epidermis and 0.30–0.35 mm particles used for the inner core. The spatial coordinate positioning method ensured regular particle arrangement and prevented particle overlap.
3. A stepwise calibration strategy combining Plackett–Burman screening, steepest ascent tests, and Box–Behnken response surface methodology was applied to identify and optimize the key bonding and contact parameters. Four bonding parameters significantly affecting shear force and five contact parameters significantly affecting the angle of repose were screened. The shear force and repose angle response surface models showed good fitting performance, with R^2 values of 0.9036 and 0.9773, respectively.
4. An FNN-based shear force prediction model was further established using the significant parameters identified by response surface analysis. The model achieved a fitting equation of $y = 0.9526x + 2.6381$, with $R^2 = 0.9077$ and RMSE = 0.9407, indicating its ability to capture the nonlinear relationship between key parameters and shear force.
5. Validation results showed that the simulated angle of repose was 31.46°, with a relative error of only 0.51%. These results confirm the accuracy and feasibility of the proposed double-layer bonded DEM model and the calibrated parameters. The modelling and calibration framework developed in this study provides a reliable reference for DEM modelling of herbaceous crop stems and for the simulation-based optimization of alfalfa harvesting machinery.

Data availability

The data that support the findings of this study are available on request from the corresponding author under reasonable request.

References

1. Gao, X.; Xuan, C.; Tang, Z.; et al. A Dynamic Drying Process: Mathematical Modeling and Energy Consumption Optimization of Alfalfa Bales Using Hot Air Drying. *Renewable Energy*, **246**, 122961. https://doi.org/10.1016/j.renene.2025.122961 (2025).
2. Zhang, W.; Cen, H.; Guo, W.; et al. A Review of Alfalfa Drying Technology and Equipment Throughout the Whole Process. *Appl. Sci*, **15**, 12268 (2025). https://doi.org/10.3390/app152212268
3. Li, Z.; Wang, Y.; Liu, J.; et al. The Potential Role of Alfalfa Polysaccharides and Their Sulphated Derivatives in the Alleviation of Obesity. *Food Funct*, **14**, 7586–7602(2023).
4. Nalawade, R. D.; Singh, K. P.; Roul, A. K.; et al. A. Study on the Effect of Geometrical and Operational Parameters on Performance Dynamics of Modified Rotary Blades Using DEM. *Sci. Rep*, **14,** 19239. https://doi.org/10.1038/s41598-024-69803-8(2024).
5. Leblicq, T.; Smeets, B.; Vanmaercke, S.; et al. A Discrete Element Approach for Modelling Bendable Crop Stems. Comput. *Electron. Agric*, **124**, 141–149(2016).
6. Bai, H.; Wu, Y.; Ma, Y.; et al. Discrete Element Model Construction and Dehulling Simulation Verification Based on Harvested Quinoa Grains. *J. Food Sci*, **89**, 9336–9353(2024).
7. Mousaviraad, M.; Tekeste, M. Z. Systematic Calibration and Validation Approach for Discrete Element Method (DEM) Modeling of Corn under Varying Moisture Contents (MC). *J. ASABE*, **67**, 259–274. https://doi.org/10.13031/ja.14763 (2024).
8. Liu, Y.; Zhao, J.; Yin, B.; et al. Discrete Element Modelling of the Yam Root–Soil Complex and Its Verification. *Biosyst. Eng*, **220**, 55–72. https://doi.org/10.1016/j.biosystemseng.2022.05.002 (2022).
9. Tong, S.; Shao, M.; Cao, M.; et al. Parameter Calibration of Discrete Element Model for Corn Stalk Based on DEM. *Chin. J. Agric. Mech*, **44**, 69–75(2023)..
10. Liu, Y.; Zhang, F.; Song, X.; et al. Study on Mechanical Properties for Corn Straw of Double-Layer Bonding Model Based on Discrete Element Method. *J. Northeast Agric. Univ*, **53**, 45–54(2022).
11. Yang, J.; Lei, J.; Qin, X.; et al. Calibration and Establishment for the Discrete Element Simulation Parameters of Pepper Stem during Harvest Period. *Sci. Rep*, **15**, 21143(2025). https://doi.org/10.1038/s41598-025-07931-5.
12. Guo, H.; Guo, L.; Li, H.; et al. Calibration and Experiment of Discrete Element Simulation Parameters for Rapeseed Stalks at the Suitable Harvest Stage. *Trans. Chin. Soc. Agric. Eng*, **40**, 20–29(2024).
13. Xie, W.; Peng, L.; Jiang, P.; et al. Discrete Element Model Building and Optimization of Double-Layer Bonding of Rape Shoots Stems at Harvest Stage. *Trans. Chin. Soc. Agric. Mach*, **54**, 112–120(2023).
14. Shi, R.; Dai, F.; Zhao, W.; et al. Establishment of Discrete Element Flexible Model and Verification of Contact Parameters of Flax Stem. *Trans. Chin. Soc. Agric. Mach*, **53**, 146–155(2022).
15. Zhao, X.; Bai, H.; Liu, F.; et al. DEM Modelling Methods and Trait Analysis of Sunflower Seed. *Biosyst. Eng*, **250**, 39–48(2025). https://doi.org/10.1016/j.biosystemseng.2024.11.012.
16. Yang, L.; Chen, W.; Kan, Z.; et al. Parameter Calibration for Discrete Element Simulation of Leymus chinensis Seeds Based on RSM Optimization. *Sci. Rep*, **15**, 7947(2025). https://doi.org/10.1038/s41598-025-89181-z.
17. Yan, D.; Yu, J.; Wang, Y.; et al. Measurement and Calibration of DEM Parameters of Soybean Seed Particles. *Agriculture*, **12**, 1825(2022). https://doi.org/10.3390/ agriculture12111825.
18. Han, D. D.; Wang, Q.; Wang, Y. X.; et al. Determination and Parameters Calibration of the Soybean-Bonded Particle Model Based on Discrete Element Method. *Comput. Part. Mech*, **12**, 231–244(2025). https://doi.org/10.1016/j.compag.2022.107502.

19. Zhao, W.; Chen, M.; Xie, J.; et al. Discrete Element Modeling and Physical Experiment Research on the Biomechanical Properties of Cotton Stalk. *Comput. Electron. Agric*, **204**, 107502(2023). http://dx.doi.org/10.1016/j.compag.2016.02.018.
20. Leblicq, T.; Smeets, B.; Ramon, H.; et al. A Discrete Element Approach for Modelling the Compression of Crop Stems. *Comput. Electron. Agric*, **123**, 80–88(2016). https://doi.org/10.1016/j.compag.2023.108283.
21. Sun, K.; Yu, J.; Zhao, J.; et al. A DEM-Based General Modeling Method and Experimental Verification for Wheat Plants in the Mature Period. *Comput. Electron. Agric*, **214**, 108283(2023). https://doi.org/10.1016/j.compag.2022.106722.
22. Li, X.; Du, Y.; Liu, L.; et al. Research on the Constitutive Model of Low-Damage Corn Threshing Based on DEM. *Comput. Electron. Agric*, **194**, 106722(2022). https://doi.org/10.1016/j.compag.2021.106349
23. Adajar, J. B.; Alfaro, M.; Chen, Y.; et al. Calibration of Discrete Element Parameters of Crop Residues and Their Interfaces with Soil. *Comput. Electron. Agric*, **188**, 106349(2021). https://doi.org/10.1016/j.biosystemseng.2021.10.010.
24. Schramm, M.; Tekeste, M. Z. Wheat Straw Direct Shear Simulation Using Discrete Element Method of Fibrous Bonded Model. *Biosyst. Eng*, **213**, 1–12(2022). doi:10.1016/j.powtec.2009.02.009.
25. Chevanan, N.; Womac, A. R.; Bitra, V. S. P.; et al. Sokhansanj, S. Flowability Parameters for Chopped Switchgrass, Wheat Straw and Corn Stover. *Powder Technol*, **193**, 79–86(2009).
26. Hao, J.; Long, S.; Li, H.; et al. Development of Discrete Element Model and Calibration of Simulation Parameters for Mechanically Harvested Yam. *Trans. Chin. Soc. Agric. Eng*, **35**, 34–42(2019).
27. Chen, T.; Yi, S.; Li, Y.; et al. Establishment of Discrete Element Model and Parameter Calibration of Alfalfa Stem in Budding Stage. *Trans. Chin. Soc. Agric. Mach*, **54**, 91–100(2023).
28. Zhao, C.; Han, Z.; Cao, Z.; et al. Experiment and Research on Mechanical Properties and Microstructure of Stems of Tangled Forage legumes at Fruiting Stage. In Proceedings of the 2010 International Agricultural Engineering Conference, Shanghai, China, 17–20 Sep (2010).
29. Potyondy, D. O.; Cundall, P. A. A Bonded-Particle Model for Rock. *Int. J. Rock Mech. Min. Sci*, **41**, 1329–1364(2004). doi:10.1016/j.powtec.2009.02.009. doi:10.1016/j.powtec.2009.02.009.
30. Hu, Y.; Xiang, W.; Duan, Y.; et al. Calibration of Ramie Stalk Contact Parameters Based on the Discrete Element Method. *Agriculture*, **13**, 1070(2023). https://doi.org/10.3390/agriculture13051070.
31. Zhang, J.; Wang, J.; Du, D.; et al. Optimization and Validation of Root-Cutting Device for Chinese Cabbage Harvester Based on Discrete Element Method. *Comput. Electron. Agric*, **214,** 108314(2023). https://doi.org/10.1016/j.compag.2023.108314.
32. Tian, Y.; Zeng, Z.; Gong, H.; et al. Simulation of Tensile Behavior of Tobacco Leaf Using the Discrete Element Method (DEM). *Comput. Electron. Agric*, **205**, 107570(2023). https://doi.org/10.1016/j.compag.2022.107570.
33. Su, Y.; Xu, Y.; Cui, T.; et al. Determination and Interpretation of Bonded-Particle Model Parameters for Simulation of Maize Kernels. *Biosyst. Eng*, **210**, 193–205(2021). https://doi.org/10.1016/j.biosystemseng.2021.08.022.
34. Liu, W.; Su, Q.; Fang, M.; et al. Parameters Calibration of Discrete Element Model for Corn Straw Cutting Based on Hertz–Mindlin with Bonding. *Appl. Sci*, **13**, 1156(2023). https://doi.org/10.3390/app13021156.
35. Zhang, T.; Zhao, M.; Liu, F.; et al. A Discrete Element Method Model of Corn Stalk and Its Mechanical Characteristic Parameters. *BioResources*, **15**, 9337–9350(2020). DOI: 10.15376/biores.15.4.9337-9350.
36. Si, S.; Zhang, B.; Huang, J.; et al. Bending Mechanics Test and Parameters Calibration of Ramie Stalks. *Sci. Rep*, **13**, 8666(2023). https://doi.org/10.1038/s41598-023-35469-x.

Author Contributions

Conceptualization, W.Z. and H.C.; methodology, W.Z. and W.G.; investigation, P.S.; resources, P.S.; data curation, W.Z. and P.S.; writing—original draft preparation, W.Z.; writing—review and editing, W.Z.; visualization, W.Z.; supervision, H.C.; project administration, W.Z. and H.C.; funding acquisition, W.Z. and W.G. All authors have read and agreed to the published version of the manuscript.

Funding

This research was funded by Natural Science Foundation of Inner Mongolia Autonomous Region, Grant No. 2025LHMS03030; Central Government Guidance Funds for Local Science and Technology Development, Grant No. 2024ZY0110; Basic Scientific Research Funds for Universities Directly Affiliated with the Inner Mongolia Autonomous Region, Grant No. ZYT2026112.

Competing interests

The authors declare no conflicts of interest.

Additional information

Correspondence and requests for materials should be addressed to W.Z. or H.T.C.

Disclaimer/Publisher's Note: The statements, opinions and data contained in all publications are solely those of the individual author(s) and contributor(s) and not of MDPI and/or the editor(s). MDPI and/or the editor(s) disclaim responsibility for any injury to people or property resulting from any ideas, methods, instructions or products referred to in the content.